

Oxygen saturation and blood-volume derivation from multi-wavelength time-resolved optical tomography data.

Elizabeth M. C. Hillman, Simon. R. Arridge[†], Jeremy C. Hebden, David T. Delpy.

University College London, Department of Medical Physics and Bioengineering, Shropshire House, 11-20 Capper Street, London WC1E 6JA UK
Tel (+44) 20 7679 6409, Fax (+44) 207 679 6269, ehillman@medphys.ucl.ac.uk

[†]University College London, Department of Computer Science, Gower Street, London WC1E 6BT, UK

Abstract: We present an analysis of the accuracy of oxygen saturation and blood volume maps derived from temporal optical tomographic data. Simulations and then clinical data are used to demonstrate different techniques for extracting the parameters.

©2001 Optical Society of America

OCIS codes: (170.6900) Tomography; (170.6920) Time resolved imaging

1. Introduction

The ultimate goal of near infrared tomography is to produce 3D images of the functional characteristics deep within volumes of tissue. The applications that we are investigating are imaging of the neonatal brain and the adult breast. Maps of the *static* oxygen saturation and blood volume along with the scattering properties of a neonatal brain would allow rapid evaluation of cerebral perfusion. A premature infant, or a term infant that has experienced birth asphyxia may have infarcts, deformities, hemorrhages or general poor control over cerebral hemodynamics that may cause regions of the brain to be starved of oxygen for long periods. Identifying regions of low perfusion would allow treatments to be developed that could prevent resultant permanent disabilities such as cerebral palsy. In breast imaging, the functional and scattering characteristics of lesions will help to distinguish between benign cysts and fibroadenomas and malignant highly vascularised tumors or necrotic regions.

Images of *changes* in saturation and blood volume would also provide useful information. In the case of the neonate, the response to treatment could be monitored, and response to artificially induced changes in cerebral perfusion could be used to evaluate hemodynamic integrity. Images of changes in saturation and volume are reported in [1].

The MONSTIR system is a 32 channel time-resolved near infrared imaging system [2]. A recently added dual cavity fiber laser (IMRA America, Inc.) can produce 40MHz pulses at 780nm and 815nm. These pulses can be interlaced as shown in Fig. 1, such that time-resolved data acquired in a 25ns window will consist of one temporal point spread function (TPSF) for 780nm and an additional TPSF for 815nm. This method of simultaneously acquiring dual wavelength information was recently demonstrated on a 30 week gestation neonate as shown in Fig. 1.

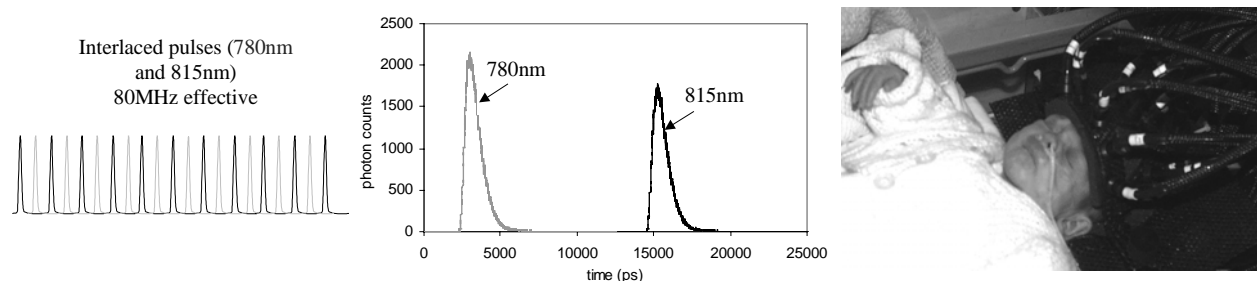


Fig. 1 (left) Interlacing pulses from two fiber lasers to create a dual wavelength pulse train (right) measurements on a 30 week gestation neonate.

Traditionally, optical tomography data has been used to reconstruct images of absorption and scatter [3] by either linear or non-linear methods. But pixel-wise quantitation of images is never going to be 100% accurate since low spatial resolution is an unavoidable feature of images reconstructed from measurements of diffuse light. In order to derive parameters such as saturation from optical tomography data we must therefore consider how to combine multi-wavelength data, and ascertain whether functional results obtained from clinical data are likely to be realistic.

2. Deriving saturation

We define fractional oxygen saturation S and fractional blood volume V of a tissue as:

$$S = \frac{[HbO_2]}{[HbO_2] + [Hb]} \quad V = \frac{\text{volume of whole blood in tissue}}{\text{total tissue volume}} \quad (1)$$

where [Hb] denotes the deoxy-hemoglobin, and [HbO₂], the oxy-hemoglobin concentration. Assuming constant hematocrit, we can express the absorption coefficient of a tissue at a particular wavelength in the following way:

$$\begin{aligned} \mu_{a,\lambda_1} &= (1-V)\mu_{a,bg,\lambda_1} + V(\mathcal{E}_{HbO_2,\lambda_1}S + (1-S)\mathcal{E}_{Hb,\lambda_1}) \\ \mu_{a,\lambda_2} &= (1-V)\mu_{a,bg,\lambda_2} + V(\mathcal{E}_{HbO_2,\lambda_2}S + (1-S)\mathcal{E}_{Hb,\lambda_2}) \end{aligned} \quad (2)$$

where $\mathcal{E}_{HbO_2,\lambda_1}$ is the molar extinction coefficient of 100% oxygenated whole blood at wavelength λ_1 and μ_{a,bg,λ_1} is the absorption coefficient of the exsanguinated tissue at λ_1 . So from Equation 2 we can derive expressions for S and V in terms of μ_{a,λ_1} , μ_{a,λ_2} , μ_{a,bg,λ_1} and μ_{a,bg,λ_2} . For simplicity we assume that $\mu_{a,bg,\lambda_1} \approx \mu_{a,bg,\lambda_2}$ i.e. the spectral variation between 780 and 815nm in the background absorption is negligible compared to the changes associated with blood.

$$S = \frac{(\mu_{a,\lambda_1} - \mu_{a,\lambda_2} + \mathcal{E}_{Hb,\lambda_2} - \mathcal{E}_{Hb,\lambda_1})\mu_{a,bg} - \mathcal{E}_{Hb,\lambda_2}\mu_{a,\lambda_1} + \mathcal{E}_{Hb,\lambda_1}\mu_{a,\lambda_2}}{(\mathcal{E}_{HbO_2,\lambda_2} - \mathcal{E}_{Hb,\lambda_2})(\mu_{a,\lambda_1} - \mu_{a,bg}) - (\mathcal{E}_{HbO_2,\lambda_1} - \mathcal{E}_{Hb,\lambda_1})(\mu_{a,\lambda_2} - \mu_{a,bg})} \quad (3)$$

$$V = 1 + \frac{\mathcal{E}_{Hb,\lambda_2}\mathcal{E}_{HbO_2,\lambda_1} - \mathcal{E}_{Hb,\lambda_1}\mathcal{E}_{HbO_2,\lambda_2} + \mu_{a,\lambda_1}(\mathcal{E}_{HbO_2,\lambda_2} - \mathcal{E}_{Hb,\lambda_2}) - \mu_{a,\lambda_2}(\mathcal{E}_{HbO_2,\lambda_1} - \mathcal{E}_{Hb,\lambda_1})}{\mathcal{E}_{Hb,\lambda_1}\mathcal{E}_{HbO_2,\lambda_2} - \mathcal{E}_{Hb,\lambda_2}\mathcal{E}_{HbO_2,\lambda_1} + \mu_{a,bg}(\mathcal{E}_{Hb,\lambda_2} - \mathcal{E}_{Hb,\lambda_1} + \mathcal{E}_{HbO_2,\lambda_1} - \mathcal{E}_{HbO_2,\lambda_2})} \quad (4)$$

This means that we will need an estimate of the absorption of the exsanguinated background tissues $\mu_{a,bg}$ if we are to derive V and S from μ_a .

3. Image reconstruction of saturation and blood volume heterogeneities.

A simulation was performed to test the accuracy of absolute saturation and fractional blood volume parameters derived from dual wavelength data. The optical properties of the simulation were based on the molar extinction coefficients of whole blood at 780nm and 815nm and calculated using Equation 2 with $\mu_{a,bg} = 0.01\text{mm}^{-1}$.

Forward data (meantime and intensity) were simulated using TOAST [4] on a 2D mesh, with 16 coincident evenly spaced sources and detectors, and optical properties as shown in Fig. 2. A homogenous reference state was assumed to have the same properties as region 0 for each wavelength. TOAST was used to simulate reference data and Jacobians based on each reference. No noise was added to the data. This simulation is intended to represent the best possible conditions for accurate derivation of functional parameters.

Images of μ_a and the diffusion coefficient $\kappa = 1/(3(\mu'_s + \mu_a))$ were reconstructed using a simple linear reconstruction method (using Tikhonov regularisation). The nodal values of the resulting $\mu_{a,780\text{nm}}$ and $\mu_{a,815\text{nm}}$ images were converted to absolute by adding the reference state values and were then manipulated using Equations 3 and 4 to produce the images shown in Fig. 2.

The images have clearly separated the three parameters successfully. Quantitatively, while the values found are close to those of the targets, there is still notable error in the retrieved parameters.

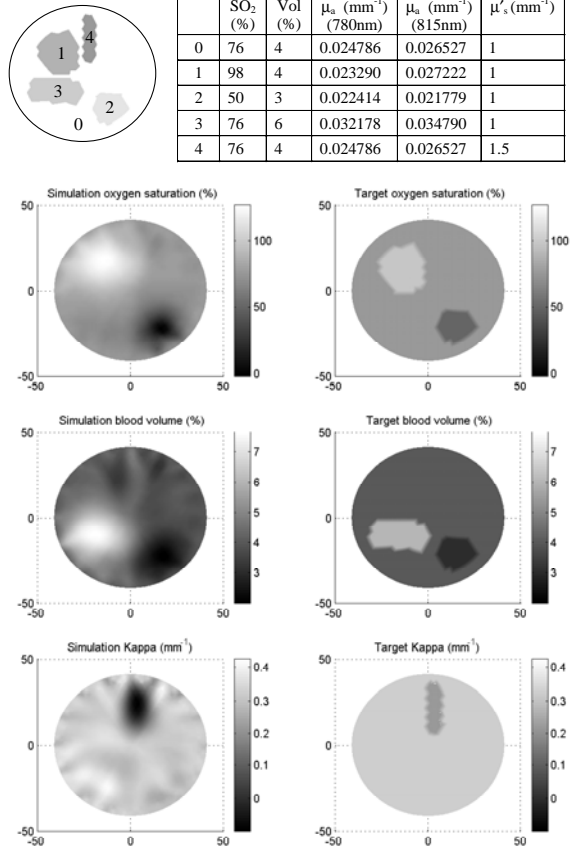


Fig. 2 Simulation to evaluate accuracy of reconstructed oxygen saturation, fractional blood volume and average kappa values.

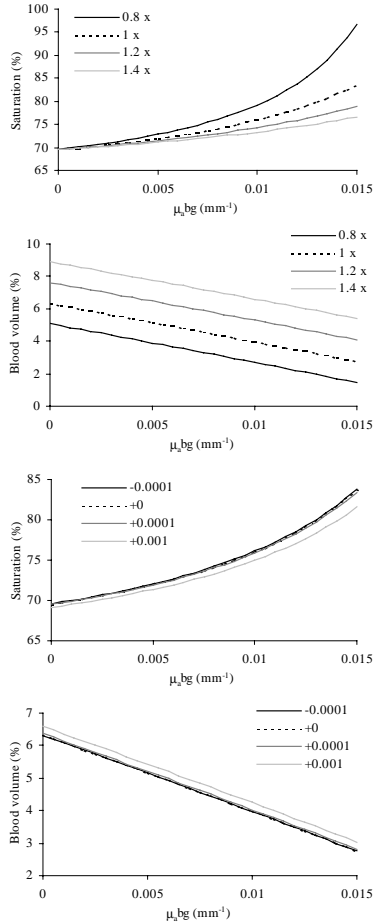


Fig. 3 Plots of the sensitivity of saturation and volume to errors in $\mu_{a,bg}$, $\mu_{a,780nm}$ and $\mu_{a,815nm}$

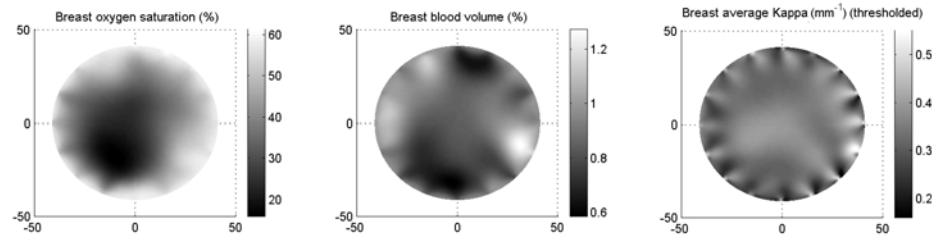


Fig. 4 Images of oxygen saturation, fractional blood volume and kappa in the breast of a healthy volunteer.

4. Summary

We have demonstrated that the accuracy of derived absolute functional parameters is likely to be affected by unavoidable errors in reconstructed absorption values. However, the techniques used have shown that saturation, blood volume and kappa can be separated using mean time and intensity dual wavelength data, and that physiological information can be deduced from clinical results. We will present the continuation of this work to more complex methods of deriving absolute, and changes in, blood saturation and volume. Constraining the solution and using combinations of input data such as the difference between two wavelengths will also be explored. These methods will be demonstrated on data recently acquired on the brain of a 30 week gestation neonate.

5. References

- [1] A. Bluestone, G. Abdoulaev, et al, "Three dimensional optical tomography of hemodynamics in the human head," *Opt. Express* **9** (6), 272-286 (2001).
- [2] F. E. W. Schmidt, M. E. Fry, E. M. C. Hillman, J. C. Hebden, and D. T. Delpy, "A 32-channel time-resolved instrument for medical optical tomography," *Rev. Sci. Instrum* **71** (1), 256 - 265 (2000).
- [3] J. C. Hebden, F. E. W. Schmidt, M. E. Fry, M. Schweiger, E. M. C. Hillman, D. T. Delpy and S. R. Arridge, "Simultaneous reconstruction of absorption and scattering images using multi-channel measurement of purely temporal data," *Optics Letters*, **24** (8), 534-536 (1999)
- [4] S. R. Arridge, M. Schweiger, " Image reconstruction in optical tomography," *Phil. Trans. Royal Soc. B* **352**, 717-726 (1997).

As can be seen from the Equations 3 and 4, absolute values of saturation will be affected by errors in $\mu_{a,bg}$, $\mu_{a,780nm}$ and $\mu_{a,815nm}$ and errors in the estimates of the extinction coefficients $\epsilon_{*,\lambda,*}$. The plots in Fig. 3 demonstrate the effect on derived saturation and volume of errors in $\mu_{a,bg}$, and (identical) additive and multiplicative errors in both $\mu_{a,780nm}$ and $\mu_{a,815nm}$. The plots were generated using the properties of region 0, with both μ_a values multiplied by 0.8, 1, 1.2 or 1.4, or with -0.0001, 0, 0.0001 or 0.001 mm^{-1} added.

The absolute functional parameters obtained are clearly very sensitive to knowledge of the background absorption, as well as to scaling errors in $\mu_{a,780nm}$ and $\mu_{a,815nm}$. Volume can become negative if too high a value of $\mu_{a,bg}$ is used, and saturation will rise until a discontinuity causes it to drop to a negative value.

2. Breast data

Fig. 4 shows images of oxygen saturation, blood volume and kappa derived from multi-wavelength data acquired on the breast of a healthy adult volunteer using MONSTIR. The same image reconstruction method as for the simulation was used. Reference data were acquired on a homogenous phantom, and Jacobians were generated based on the phantom's properties. A 2D mesh was used and the estimate that $\mu_{a,bg} = 0.003mm^{-1}$.

Structure can be seen in all three images. The saturation image implies that the central area of the breast has a low saturation compared to the areas closer to the surface. The volume image may have revealed the presence of veins running under the surface of the skin. The kappa image reveals that an area of low scatter coincides with the region of low perfusion and low blood volume.

While the simulations above have demonstrated that these results are not likely to be entirely quantitatively accurate, this method has revealed spatial heterogeneities in functional parameters within the breast.